# Giant Acoustic Concentration by Extraordinary Transmission in Zero-Mass Metamaterials

Jong Jin Park,[1] K. J. B. Lee,[2] Oliver B. Wright,[3] Myoung Ki Jung,[1] and Sam H. Lee[1,*]

[1]*Institute of Physics and Applied Physics, Yonsei University, Seoul 120-749, Korea*

[2]*Department of Physics, Ewha Womans University, Seoul 120-750, Korea*

[3]*Division of Applied Physics, Faculty of Engineering, Hokkaido University, Sapporo 060-8628, Japan*

(Received 9 October 2012; revised manuscript received 28 February 2013; published 13 June 2013)

We demonstrate 97%, 89%, and 76% transmission of sound amplitude in air through walls perforated with subwavelength holes of areal coverage fractions 0.10, 0.03, and 0.01, respectively, producing 94-, 950-, and 5700-fold intensity enhancements therein. This remarkable level of extraordinary acoustic transmission is achieved with thin tensioned circular membranes, making the mass of the air in the holes effectively vanish. Imaging the pressure field confirms incident-angle independent transmission, thus realizing a bona fide invisible wall. Applications include high-resolution acoustic sensing.

DOI: 10.1103/PhysRevLett.110.244302 PACS numbers: 43.60.Vx, 78.67.Pt, 81.05.Xj

The pioneering work by Ulrich and by Ebbesen *et al.* [1,2] on the extraordinary optical transmission (EOT) through a lattice of subwavelength holes has inspired extensive studies on the transmission properties of electromagnetic waves through tiny apertures of various shapes and decorations [3–11]. Diverse physical mechanisms responsible for EOT include surface plasmon polaritons [1–8], waveguide modes [9], and dynamic diffraction [10]. In the case of acoustic waves, extraordinary transmission was predicted by Zhang [11] and first reported by Lu *et al.* in gratings [12]. More recently, several groups have measured the transmission properties of sound through plates with slits and holes [13–18]. Three types of transmission mechanism were proposed for acoustic extraordinary transmission: periodic-lattice resonances, Fabry-Perot–type resonances, and elastic Lamb-mode resonances.

Independent of the mainstream EOT development, Silveirinha and Engheta [19] theoretically demonstrated, and it was soon after experimentally verified [20], that electromagnetic supercoupling and enhanced energy flux can be obtained using subwavelength channels in (dielectric constant) epsilon-near-zero materials. Since the phase velocity of an epsilon-near-zero material is extremely large, one can posit the existence of a similar supercoupling effect in acoustic metamaterials with a huge effective sound velocity; such acoustic media require either the compressibility or the density to be almost zero [21]. Here we propose a recipe for an acoustic metamaterial in the form of a rigid plane containing holes that give zero effective mass for the air therein. To achieve this we make use of holes containing tightly stretched membranes and demonstrate by both theory and experiment an unprecedentedly efficient extraordinary transmission of sound through the perforated wall.

A rigid wall reflects sound because no volume flow of air is allowed across it. Perforating it with very small holes does not increase the volume flow appreciably because of the large inertance (i.e., the equivalent of inertia for sound waves) of the air column set in motion in the hole, and most of the acoustic intensity is still reflected. Our proposed new mechanism for extraordinary transmission involves making the effective mass of the air column disappear by introducing a thin membrane. Metamaterials consisting of arrays of thin membranes were reported to exhibit tunable density [22–27]. We therefore install tensioned membranes across the holes, so that the air column and membranes form a metamaterial structure equivalent to a unit cell of the system described in Refs. [23,24].

We first derive the transmission characteristics of plane waves at normal incidence on a perforated wall by matching the pressure $p$ and the particle velocity $u$ on both sides under the assumption that the radius $r$ of the holes and the thickness $w$ of the wall are very small compared to the acoustic wavelength $\lambda$. The hole separation $d$ is assumed to be sufficient to avoid interaction effects between adjacent holes. Let $p_i$, $p_r$, $p_t$ and $u_i$, $u_r$, $u_t$ denote the pressure- and particle-velocity amplitudes for normally incident plane sinusoidal waves, where the subscripts $i$, $r$, and $t$ denote incident, reflected, and transmitted, respectively. Except for the regions inside and in the near field of the holes, the pressure- and particle-velocity amplitudes $p_1$, $u_1$ on the input (left-hand) side of the wall are given by $p_1 = p_i + p_r$ and $u_1 = u_i + u_r$. Those for the output (right-hand) side of the wall are $p_2 = p_t$ and $u_2 = u_t$. Pressures and particle velocities are related by the impedance $Z_0 = \sqrt{\rho_0 B_0}$, where $\rho_0$ and $B_0$ are the density and bulk modulus of air, respectively: $p_i = Z_0 u_i$, $p_r = -Z_0 u_r$, and $p_t = Z_0 u_t$ [24]. According to a lumped-element description of the system [28], we shall define effective mass $M_{\rm eff}$ and damping coefficient $b_{\rm eff}$ of a hole in terms of the relation

$$(p_1 - p_2)\pi r^2 = M_{\rm eff}\ddot{\xi} + b_{\rm eff}\dot{\xi}, \qquad (1)$$

where $\xi$ is the average displacement of the air column in each hole. This expression is applicable for both bare and membrane-covered holes.

 

Here we confine our geometry to $w, r, d \ll \lambda$. Therefore the effective length of the air column $l' \approx w + 1.7r$ [28] is small compared to the wavelength (i.e., $l' \ll \lambda$), and it is not necessary to consider internal (vibrational) motion of the air column. Contrary to the present case, Fabry-Perot–type acoustic extraordinary transmission requires $l' \sim \lambda$. In that case, Eq. (1) is applicable for the motion of the center of mass of the air column, and more equations are needed to describe the internal motion and standing wave formation responsible for the Fabry-Perot–type extraordinary transmission [12,15–17]. In our case, the treatment is much simpler because there is no internal motion. Moreover, since the volume $\pi r^2 l'$ of the air column is so small, we can ignore the volume expansion and take $u_1 = u_2$, $u_i + u_r = u_t$, and $1 - R = T$, where $R$ and $T$ are pressure amplitude reflection and transmission coefficients. Equation (1), together with the harmonic expression $\xi(t) = \xi_0 \exp(-i\omega t)$, lead to

$$T = \frac{1}{1 + \frac{A}{2Z_0 \pi^2 r^4}(b_{\text{eff}} - i\omega M_{\text{eff}})}, \tag{2}$$

where $A$ is the area of a metamaterial unit cell, or, for the case of a single hole in a tube, the tube inner cross-sectional area. A more detailed derivation of Eq. (2) is given in the Supplemental Material [29].

We first tested the transmission characteristics of a one-hole rigid circular wall with the setup of Fig. 1(a). Midway along a circular tube of length 2.3 m and 100-mm inner diameter we set a 5-mm thick aluminum wall with a 17-mm diameter hole at its center. This corresponds to a filling factor (i.e., areal coverage fraction) $\alpha = \pi r^2 / A = 0.03$. Tunable single-tone kHz sound ($\lambda \sim 0.3$ m) was sent from the loudspeaker at one end of the tube to measure $T$ and $R$ at normal acoustic incidence.

With the hole open (without the membrane), we measured only 3.5% of the incident acoustic intensity passing through, as shown by the open triangles in Fig. 1(b). This figure also shows the theoretical prediction (dashed curve) from Eq. (2). We used $M_{\text{eff}} = M_{\text{air}} = \pi r^2 l' \rho_0$, where $l' = w + 2\Delta l$ is the effective length of the air column with the end correction $\Delta l \approx 0.85r$ [28]. This approximation gradually becomes worse as the filling fraction $\alpha$ increases, as can be seen by considering the extreme case $\alpha = 1$, i.e., that of no wall (where $\Delta l = 0$). A better approximation is the use of $\Delta l = \zeta r$, with the parameter $\zeta$ chosen to be an appropriate monotonically decreasing function of $\alpha$. Rayleigh [30] demonstrated theoretically that $\zeta$ also has a weak dependence on the ratio $w/r$: in the case $\alpha \ll 1$, $\zeta$ varies from 0.785 ($w/r \ll 1$) to 0.849 ($w/r \gg 1$). Our choice $\zeta = 0.85$ produces a reasonable fit to our bare-hole experiment with $w/r = 0.6$ and $\alpha = 0.03$.

The damping coefficient is $b_{\text{eff}} = b_{\text{air}} \approx 2\pi r l' (\rho_0 \omega \delta / 4)$, where $\delta$ is the viscous skin depth ($\delta / r \approx 0.008$) [31]. The damping coefficient $b_{\text{air}}$ is much smaller than the inertia term $\omega M_{\text{air}}$, and $b_{\text{air}}$ can thus be neglected (to better than 1% accuracy).

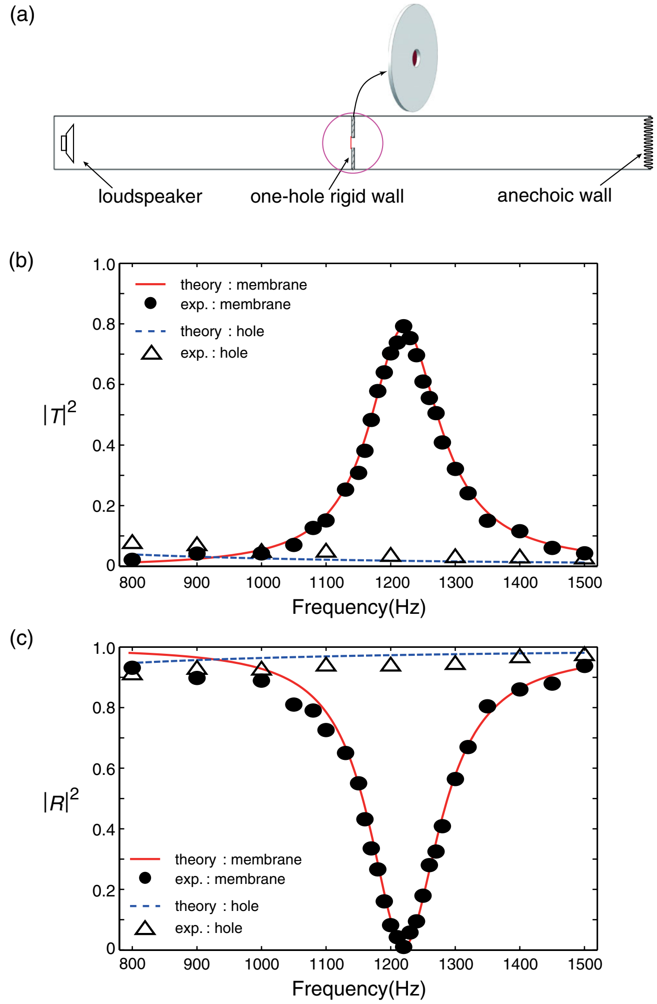


FIG. 1 (color online). (a) Setup. A probe microphone near the tube walls probes the pressure. (b) Transmission intensity coefficient $|T|^2$. (c) Reflection intensity coefficient $|R|^2$.

When we install a 0.01-mm thick low density, $920\ \text{kg/m}^3$, polyethylene tensioned membrane $|T|^2$ increases to a maximum of 79% (or $T \approx 0.9$) at the resonance frequency of 1.22 kHz (see solid circles). Apart from the presence of dissipation that slightly reduces the transmission, at this frequency the wall is close to being invisible. The restoring force from the membrane adds a negative term to the effective mass: $M_{\text{eff}}(\omega) = M_{\text{air}} + M_{\text{mem}} - k/\omega^2$ [23], where $M_{\text{mem}}$ and $k$ are the mass and spring constant of the membrane, respectively. [Equation (2) for this case becomes a low-frequency approximation to a more general relation given in Ref. [22].] At resonance, $\omega_0 = \sqrt{k/(M_{\text{air}} + M_{\text{mem}})}$, the effective mass, the dominant term in the parenthesis in Eq. (2) at other frequencies, becomes zero, and $T$ is significantly enhanced. (The condition for zero $M_{\text{eff}}$ is graphically represented in the Supplemental Material [29].) When the $M_{\mathrm{eff}}$ term disappears, $T$ is governed by $b_{\mathrm{eff}}$. Rather than theoretically determining the damping $b_{\mathrm{eff}} = b_{\mathrm{air}} + b_{\mathrm{mem}}$, we extract it from the experimental value of transmission coefficient at the resonance frequency of 1.22 kHz, $T_{\mathrm{res}} \approx 0.89$, using the relation $b_{\mathrm{eff}} = (2Z_0\pi^2 r^4/A)(T_{\mathrm{res}}^{-1} - 1)$ derived from Eq. (2). This yields $b_{\mathrm{eff}} = 6.7 \times 10^{-4}$ kg/s. The excellent agreement of the theoretical curve–using the measured $\omega_0$ but no further adjustable parameters—with experiment in Fig. 1(b) (solid curve) supports this approach. (An expression for the $Q$ factor of the resonance is derived in the Supplemental Material [29].)

Figure 1(c) shows the corresponding reflection data for $|R|^2$ and theoretical fits obtained using $R = 1 - T$, showing good agreement with experiment. On resonance, most of the acoustic energy is strongly reflected from the wall with the hole, but with the membrane in place no detectable reflection was observed; much of the incident energy is funneled into the small hole covering only 3% of the wall area, giving a particle velocity inside the holes 31 times greater than that of the incident wave. In other words, there is a ($|T|^2/\alpha^2 \approx 950$)-fold energy density intensification in the hole. Since the hole areal coverage affects the wave energy concentration in the hole, we tried a smaller, 10-mm diameter hole in an otherwise identical setup with filling factor $\alpha = 0.01$. At a resonance at 1.22 kHz we observed a 6% reflection and a 57% transmission in terms of intensity (76% in amplitude). Even though we lose 37% of the energy to viscous losses, the particle-velocity enhancement increases to 76 and the energy density intensification to 5700. This remarkably high experimental value is around 2 orders of magnitude better than the previous record in acoustics [12]. The use of a zero effective mass stemming from the membrane has greatly improved the efficiency.

Having verified the zero-mass principle with a single hole, we turn to the case of a metamaterial consisting of a periodic hole array. From the symmetry of the setup, the normally incident plane waves are expected to remain plane on transmission to the acoustic far field. To experimentally confirm this, we constructed an array of four holes drilled along the bisecting line of a rectangular rigid acrylic plate of thickness 5 mm, as shown in Fig. 2(a), placed in a rectangular cross-sectional duct. This setup accommodates two-dimensional (2D) plane waves generated by an array of four speakers at the duct entrance, as can be seen from top-view schematics in Fig. 2(a). The filling factor of the four-hole plate, $\alpha = 0.03$, was fixed by the choices $r = 8.5$ and $d = 88.6$ mm, respectively, where $d$ is the array period. The wall was first installed perpendicular to the direction of incidence (incidence angle $\theta = 0°$). Figure 2(b) shows the measured instantaneous 2D pressure distributions at 1.20 kHz for the three cases of no wall, wall with bare holes, and perforated wall with resonantly vibrating membrane-covered holes (from top to bottom, respectively), obtained using a scanned probe

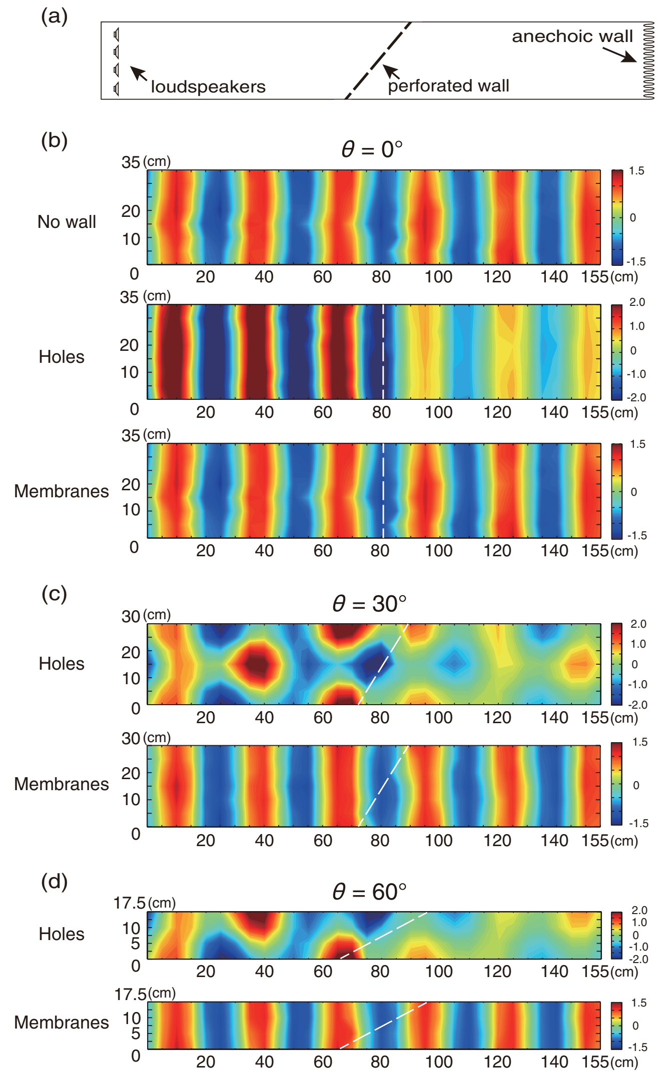


FIG. 2 (color online). (a) Setup (top view). (b) Images (interpolated from 2D arrays of points on square lattices—32 points along the duct axis) of the instantaneous pressure distribution at 1.2 kHz for no wall, a perforated wall with bare holes, and a wall with otherwise identical membrane-covered holes. (c) Images for the case of a perforated wall for acoustic incidence at $\theta = 30°$. (d) Equivalent images for $\theta = 60°$.

microphone near the top of the duct. The wall with the bare holes seriously hinders the transmission, but with the membrane installed the transmission becomes, as expected, almost as good as with no wall. Our plane-wave assumption is also borne out by this data. Since the microphone at the top of the duct is located about 40 mm above the holes, near-field variations are not apparent even when it scanned along a line close to the wall.

Following similar experiments in plasmonics and acoustics, Fig. 2(c) compares the measured transmission of the perforated walls installed for the case of a nonzero angle of incidence, here $\theta = 30°$, for both bare holes and membrane-covered holes. It is evident that the strong oblique reflection in the case of bare holes results in a

TABLE I. Transmission and reflection data for the six combinations shown in Fig. 2. $\theta$ is the angle of incidence.

| | Holes with membranes | | | Bare holes | | |
|---|---|---|---|---|---|---|
| $\theta$ | 0° | 30° | 60° | 0° | 30° | 60° |
| $\lvert T\rvert^2$ | 0.81 | 0.81 | 0.83 | 0.09 | 0.09 | 0.14 |
| $\lvert R\rvert^2$ | 0.003 | 0.005 | 0.002 | 0.82 | 0.78 | 0.72 |

complicated interference pattern. In contrast, the membrane-covered holes show no such pattern, somewhat astonishingly, owing to negligible reflections from the tilted wall under otherwise identical conditions to the normal-incidence case. Moreover, the wave is again transmitted almost as if the wall were not present. Figure 2(d) shows a similar experimental result for $\theta = 60°$. The experimentally determined $|T|^2$ and $|R|^2$ for the six investigated cases are listed in Table I, demonstrating excellent transmission when the membranes are installed. Clearly the fixed membrane resonance frequency involved in our zero-mass metamaterial enables this incident-angle independence. This presents a significant advance compared to other extraordinary acoustic transmission investigations that all involve angle-dependent resonances [12,16,17] (arising from $\lambda \sim d$).

The experimental data shown in Fig. 2 suggest that on resonance the perforated wall with membranes should be effectively invisible for any incident angle $\theta$, implying that an arbitrarily shaped wave front should also be efficiently transmitted. To verify this for the case of diverging waves, we constructed a 2D rectangular space containing a point source and a brass wall of thickness 3 mm perforated by a line of holes arranged along its bisecting line. Top and bottom containing plates of dimensions $900 \times 740$ mm$^2$ are placed parallel and 20 mm apart, and are blocked at the edges by anechoic walls. Figure 3 shows top views of the instantaneous pressure distributions at 1.9 kHz for the cases of no wall and a wall with 37 membrane-covered holes of radius $r = 3.5$ mm and separation $d = 20$ mm ($\alpha = 0.10$, with $T = 0.97$ and 94-fold energy density intensification in the holes determined from separate resonant plane-wave experiments). It is clear that, on resonance, the wave from the point source propagates unhindered by the wall, rendering it effectively invisible for acoustic waves at any incident angle.

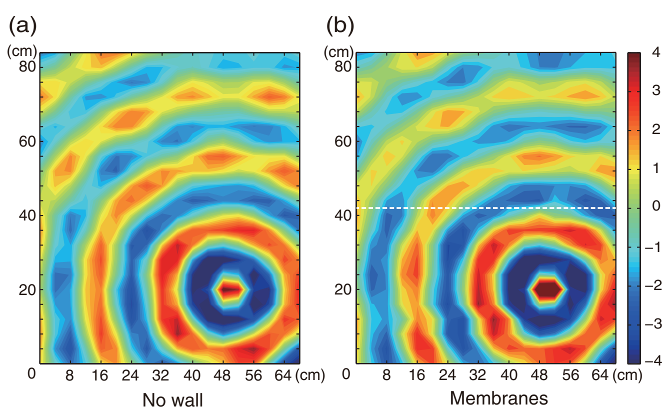


FIG. 3 (color online). (a) Pressure distributions from a point source with no wall in the middle. (b) Corresponding image when a perforated wall with membranes is installed. Data were collected in the same way as for Fig. 2, here on a square lattice of points of separation 40 mm.

In conclusion, we realize zero-mass metamaterials by making the inertance of membrane-covered air holes close to zero. We thereby experimentally and theoretically demonstrate a new mechanism for acoustic extraordinary transmission. For a filling fraction of 3% we observe, on resonance, that 79% of the incident acoustic energy in air is transmitted through the holes (89% in amplitude) while maintaining the wave propagation direction independent of the angle of incidence. For a filling fraction of 1% we obtain a 57% transmission intensity (76% in amplitude); this implies that on resonance the particle velocity inside a hole is 76 times greater than that of the incident wave, corresponding to an intensification of the acoustic energy density by the giant factor of 5700. Such a high concentration of acoustic energy into a small hole of radius $r = \lambda/56$ enables sensitive detection of acoustic signals with subwavelength resolution: in optics, such subwavelength intensity concentration is used in scanning near-field optical microscopy [3], and the present work not only opens the way to the efficient realization of its acoustic counterparts in fluid ultrasonics and underwater acoustics, but also to the analogous realization in solid-state ultrasonics.

This research was supported by the Basic Science Research Program through the National Research Foundation of Korea (NRF) funded by the Ministry of Education, Science and Technology (NRF No. 2012-0002272 and No. 2012-0000547).

*samlee@yonsei.ac.kr

[1] R. Ulrich, in *Optical and Acoustical Microelectronics*, edited by J. Fox (Polytechnic, New York, 1974), p. 359.
[2] T. W. Ebbesen, H. J. Lezec, H. F. Ghaemi, T. Thio, and P. A. Wolff, Nature (London) **391**, 667 (1998).
[3] C. Genet and T. W. Ebbesen, Nature (London) **445**, 39 (2007).
[4] H. F. Ghaemi, T. Thio, D. E. Grupp, T. W. Ebbesen, and H. J. Lezec, Phys. Rev. B **58**, 6779 (1998).
[5] L. Martin-Moreno, F. J. Garcia-Vidal, H. J. Lezec, K. M. Pellerin, T. Thio, J. B. Pendry, and T. W. Ebbesen, Phys. Rev. Lett. **86**, 1114 (2001).
[6] J. B. Pendry, L. Martin-Moreno, and F. J. Garcia-Vidal, Science **305**, 847 (2004).
[7] D. C. Skigin and R. A. Depine, Phys. Rev. Lett. **95**, 217402 (2005).
[8] K. G. Lee and Q. H. Park, Phys. Rev. Lett. **95**, 103902 (2005).
[9] H. Liu and P. Lalanne, Nature (London) **452**, 728 (2008).

[10] M. M. J. Treacy, Appl. Phys. Lett. **75**, 606 (1999).
[11] X. Zhang, Phys. Rev. B **71**, 241102 (2005).
[12] M. H. Lu, X. K. Liu, L. Feng, J. Li, C. P. Huang, Y. F. Chen, Y. Y. Zhu, S. N. Zhu, and N. B. Ming, Phys. Rev. Lett. **99**, 174301 (2007).
[13] J. Christensen, A. I. Fernandez-Dominguez, F. Leon-Perez, L. Martin-Moreno, and F. J. Garcia-Vidal, Nat. Phys. **3**, 851 (2007).
[14] J. Christensen, L. Martin-Moreno, and F. J. Garcia-Vidal, Phys. Rev. Lett. **101**, 014301 (2008).
[15] B. Hou, J. Mei, M. Ke, W. Wen, Z. Liu, J. Shi, and P. Sheng, Phys. Rev. B **76**, 054303 (2007).
[16] H. Estrada, P. Candelas, A. Uris, F. Belmar, F. J. Garcia de Abajo, and F. Meseguer, Phys. Rev. Lett. **101**, 084302 (2008).
[17] H. Estrada, F. J. Garcia de Abajo, P. Candelas, A. Uris, F. Belmar, and F. Meseguer, Phys. Rev. Lett. **102**, 144301 (2009).
[18] J. Mei, B. Hou, M. Ke, S. Peng, H. Jia, Z. Liu, J. Shi, W. Wen, and P. Sheng, Appl. Phys. Lett. **92**, 124106 (2008).
[19] M. Silveirinha and N. Engheta, Phys. Rev. Lett. **97**, 157403 (2006).
[20] B. Edwards, A. Alu, M. E. Young, M. Silveirinha, and N. Engheta, Phys. Rev. Lett. **100**, 033903 (2008).
[21] Z. Liang and J. Li, Phys. Rev. Lett. **108**, 114301 (2012).
[22] Z. Yang, J. Mei, M. Yang, N. H. Chan, and P. Sheng, Phys. Rev. Lett. **101**, 204301 (2008).
[23] S. H. Lee, C. M. Park, Y. M. Seo, Z. G. Wang, and C. K. Kim, Phys. Lett. A **373**, 4464 (2009).
[24] S. H. Lee, C. M. Park, Y. M. Seo, Z. G. Wang, and C. K. Kim, Phys. Rev. Lett. **104**, 054301 (2010).
[25] C. J. Naify, C.-M. Chang, G. McKnight, and S. Nutt, J. Appl. Phys. **108**, 114905 (2010).
[26] C. M. Park, J. J. Park, S. H. Lee, Y. M. Seo, C. K. Kim, and S. H. Lee, Phys. Rev. Lett. **107**, 194301 (2011).
[27] C. J. Naify, C.-M. Chang, G. McKnight, F. Scheulen, and S. Nutt, J. Appl. Phys. **109**, 104902 (2011).
[28] D. T. Blackstock, *Fundamentals of Physical Acoustics* (Wiley, New York, 2000).
[29] See Supplemental Material at http://link.aps.org/supplemental/10.1103/PhysRevLett.110.244302 for detailed information on the derivation of the acoustic transmission through an array of subwavelength holes, or through a single such hole in a duct, according to a lumped element approach; this approach is also used to derive conditions for zero effective mass, as well as to obtain an analytical expression for the $Q$ factor of the membrane resonance.
[30] L. Rayleigh, *The Theory of Sound* (Dover, New York, 1945), 2nd ed., Vol. 2, pp. 180–183.
[31] M. J. Moloney, Am. J. Phys. **72**, 1035 (2004).